THE JOURNAL OF PHYSICAL CHEMISTRY A

Article

pubs.acs.org/JPCA

Electron Attachment to CO_2 Embedded in Superfluid He Droplets

Johannes Postler,[†] Violaine Vizcaino,[‡] Stephan Denifl,[†] Fabio Zappa,[§] Stefan Ralser,[†] Matthias Daxner,[†] Eugen Illenberger,*[,∥] and Paul Scheier*[,†]

[†]Institut für Ionenphysik und Angewandte Physik, Universität Innsbruck, Technikerstrasse 25, A-6020 Innsbruck, Austria

[‡]CIMAP - CEA, CNRS, ENSICAEN, UCBN, Boulevard Henri Becquerel, BP 5133, 8 14070 Caen cedex 5, France

[§]Department of Physics - ICE - University Campus - Universidade Federal de Juiz de Fora, Juiz de Fora - MG 36036-900, Brazil

[∥]Institut für Chemie, Freie Universität Berlin, Takustrasse 3, 14195 Berlin, Germany

ABSTRACT: Electron attachment to CO_2 embedded in superfluid He droplets leads to ionic complexes of the form $(CO_2)_n^-$ and $(CO_2)_nO^-$ and, at much lower intensities, He containing ions of the form $He_m(CO_2)_nO^-$. At low energies (<5 eV), predominantly the non-decomposed complexes $(CO_2)_n^-$ are formed via two resonance contributions, similar to electron attachment to pristine CO_2 clusters. The significantly different shapes and relative resonance positions, however, indicate particular quenching and mediation processes in CO_2@He. A series of further resonances in the energy range up to 67 eV can be assigned to electronic excitation of He and capture of the inelastically scattered electron generating $(CO_2)_n^-$ and two additional processes where an intermediately formed He* leads to the nonstoichiometric anions $(CO_2)_nO^-$.

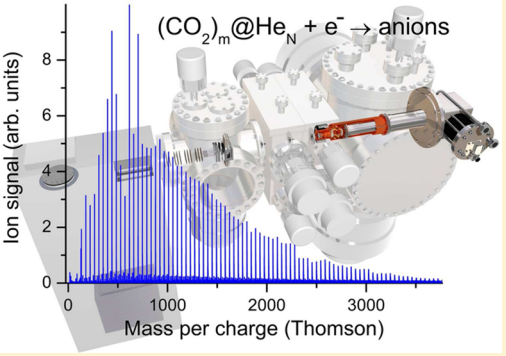

INTRODUCTION

Electron attachment to CO_2 embedded in superfluid He droplets (CO_2@He) is studied in a crossed beams experiment with mass spectrometric detection of the anions. Over the past few years electron attachment and/or electron ionization for a variety of molecules embedded in He droplets, including H_2O,[1] $CHCl_3$,[2] and more complex systems like the explosive trinitrotoluene (TNT)[3] or building blocks of life such as DNA bases[4] and amino acids[5,6] and recently also mixtures of fullerenes and various low-mass molecules[7−10] have been studied in our laboratory. It has been shown that He droplets provide excellent conditions to generate relaxed parent anions, which are not observed in free electron attachment experiments with the corresponding gas phase molecules. The general behavior for a molecule embedded in a helium droplet is that the dissipative environment suppresses dissociative electron attachment (DEA) in favor of associative attachment (AA, formation of the parent anion). In extreme cases, DEA can be suppressed completely and only intact anions are generated. This is the case, e.g., when DEA to the isolated molecule is characterized by indirect and slow reactions like in TNT.[11] In this case the rich fragmentation patterns, partly due to metastable decompositions (processes occurring on the microsecond time scale) being completely suppressed in favor of AA when going from the isolated molecule to TNT@He.[3] In addition, He droplets serve as a cryogenic nanolaboratory to study processes at temperatures close to zero K.[12]

Electron scattering from CO_2 and DEA to CO_2 has a long and interesting history owing to the fact that linear CO_2 becomes bent when attaching an electron and thereby generating CO_2^-. Interestingly, in spite of extensive research, the exact number of the most fundamental quantity connecting the ground state molecule with its anion, namely the (adiabatic) electron affinity of CO_2 (corresponding to the (adiabatic) electron binding energy of CO_2^-) is still under question. The most recent high-level *ab initio* calculations[13] predict that the O−C−O angle decreases from 180° to 138°, while the bond distance increases from 117 to 124 pm when changing from the neutral to the anion. The energy of ground state CO_2^- is predicted to be 0.6 eV *above* that of the neutral, indicating that CO_2^- is metastable and the *adiabatic* electron affinity of CO_2 is negative (−0.6 eV). On the other hand, there are hints from photodetachment spectroscopy that the electron affinity of CO_2 might be positive.[14]

Electron scattering from gas phase CO_2 exhibits a structured resonant feature centered at 3.7 eV, which is assigned as a $^2\Pi_u$ shape resonance due to accommodation of the extra electron into the lowest unoccupied molecular orbital (MO) with antibonding π^* character.[15,16] These structures are identified as symmetric stretch vibrations in the transitory anion ($CO_2^{-\#}$), also referred to as *boomerang* structures. The term boomerang is based on the idea that in the transient anion (TNI) only *one* reflection of the nuclear wave packet occurs along the symmetric stretch before it is annihilated by autodetachment. The resonance position further indicates that the vertical attachment energy (3.7 eV) is considerably larger than the

Special Issue: Franco Gianturco Festschrift

Received: March 31, 2014
Revised: May 9, 2014
Published: May 12, 2014

   dx.doi.org/10.1021/jp503179d | *J. Phys. Chem. A* 2014, 118, 6553−6559

energy to generate CO_2^- in its equilibrium geometry, which is also expected from the large geometry change between the neutral and the anion as mentioned above.

Negative ion formation in electron capture by single gas phase CO_2 yields O^- as the only observable negative ion.[17,18] The energetic threshold for O^- formation (at 300 K) is at 4.0 eV,[19] and hence DEA is energetically only accessible from the higher energy side of the $^2\Pi_u$ resonance. The further resonance contribution at 8.2 eV is due to DEA involving a core excited resonance.

More than three decades ago, CO_2 was among the first systems where negative ion formation in electron attachment to homogeneous clusters was studied. These earlier studies (at poor electron energy resolution) indicated the formation of non-decomposed complexes of the form $(CO_2)_n^-$ below 4 eV and products of the form $(CO_2)_nO^-$ within the energy domain of the $^2\Pi_u$ resonance.[20−23] Later, a study at ultrahigh resolution (1 meV, laser photoelectron attachment) revealed sharp structures in the energy range between threshold and 180 meV observed on the products $(CO_2)_n^-$.[24] These structures were identified as vibrational Feshbach resonances (VFRs) involving symmetric stretch and bending vibrations.[25] Vibrational Feshbach resonances at energies up to 0.5 eV could also be identified in a high-resolution (0.1 eV) study on electron attachment to CO_2 clusters recently performed by our laboratory.[26]

Here we explore electron attachment to CO_2@He in the energy range 0−67 eV. Under typical experimental conditions He droplets are usually doped with several molecules, which will lead to cluster formation inside the droplet and hence not only electron attachment to single CO_2 molecules but also the results from electron attachment to clusters are important for the interpretation of the present results. As will be shown, effective electron attachment takes place in the energy range below 5 eV, similar to pristine CO_2 clusters. In addition, further strong resonance features are observed in the range up to 67 eV, which can be assigned to electronic excitation of He and subsequent attachment of the slowed down electron forming $(CO_2)_n^-$ as well as a second process where an intermediate He* is colliding with the neutral CO_2 cluster and forms predominantly the nonstoichiometric ions $(CO_2)_nO^-$.

EXPERIMENTAL SECTION

The present measurements are performed with a He droplet source combined with a pickup cell containing CO_2, an ion source and a mass spectrometer system to analyze the resulting anions. The helium droplet beam is formed by expansion of He through a nozzle of 5 μm diameter into vacuum at a temperature between 8 and 13 K and a pressure of typically 23 bar. Under these operating conditions the mean size of the helium droplets is between 10^6 and 10^3. At a distance of 1 cm downstream, the He droplets pass a skimmer before they enter a differentially pumped pickup cell. About 20 cm further downstream the CO_2 doped helium droplet beam enters the collision chamber of an ion source where free electron attachment to the doped droplets takes place. In the present study we utilize either a commercial Nier-type ion source (electron energy resolution about 1 eV) in combination with an orthogonal time-of-flight mass spectrometer[7] or a home-built hemispherical electron monochromator (electron energy resolution around 100 meV) equipped with a quadrupole mass filter and channel electron multiplier.[27] The electron energy scale is calibrated by measuring the well-known narrow resonance in SF_6 close to 0 eV leading to the parent anion SF_6^- under identical conditions.

RESULTS AND DISCUSSION

For the isolated CO_2 molecule O^- is the only DEA product, which is formed via two pronounced resonances at 4.4 and 8.2 eV[26] due to the DEA reaction

$$e^- + CO_2 \rightarrow CO_2^{\#-} \rightarrow O^- + CO \quad (1)$$

with $CO_2^{\#-}$ the transient negative ion initially formed upon electron attachment. The low-energy peak is associated with the $^2\Pi_u$ shape resonance and the one at higher energy with an electronically excited Feshbach resonance. This excited resonance decomposes by releasing appreciable translational energy but also vibrational excitation in CO (up to $v = 21$).[18]

Similar to the CO_2 clusters,[20] electron attachment to CO_2@He leads to the two series of ions, namely the non-decomposed complexes of the form $(CO_2)_n^-$ ($n > 1$) and solvated fragment ions of the form $(CO_2)_nO^-$ ($n > 0$). In addition, He containing complexes of the composition $He_m(CO_2)_nO^-$ are generated.

Figure 1 displays a mass spectrum in the range between $(CO_2)_2O^-$ (104 u) and the complex $He_3(CO_2)_2O^-$ (116 u),

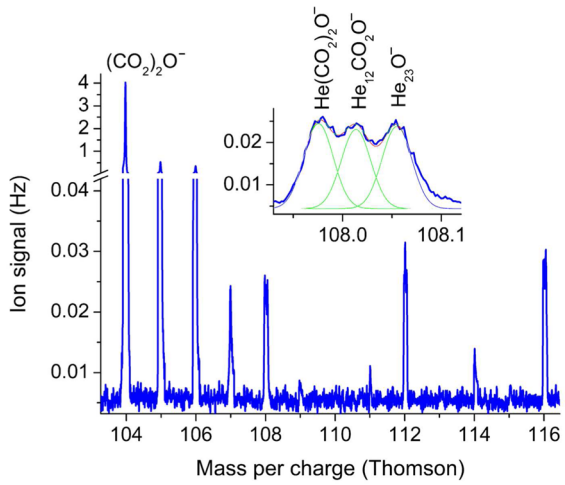

Figure 1. Section of the mass spectrum recorded with the orthogonal time-of flight instrument and low-electron-energy resolution (1 eV) obtained from electron attachment to CO_2@He recorded at an electron energy of 13 eV a stagnation pressure 23 bar and a nozzle temperature of 9.7 K. Conditions: CO_2 pressure in the pickup chamber 4.1 mPa, length of pickup region 10 cm, electron current 45 μA.

taken at an electron energy of 13 eV. The peaks at 105, 106, and 107 u are due to the isotopes ^{13}C, ^{17}O, and ^{18}O in $(CO_2)_2O^-$. A series of peaks at appreciably lower intensity than the $(CO_2)_2O^-$ is visible, which can be assigned to ions of the form $He_m(CO_2)_nO^-$ ($n = 0−2$ and $m = 1,2,3 + 11(2 - n)$). The mass resolution $m/\Delta m$ of roughly 3000 (FWHM) enables us to resolve triplets at 108, 112, and 116 u, which can be assigned to three anions where 11 He atoms replace one CO_2 unit. The inset shows a three-Gaussian-fit to the mass peak at 108 u. It is interesting to note that the yield of the He containing anionic complexes is not decreasing noticeably up to about 20 He atoms. A tightly bound shell of He, often referred to as a snowball is expected to lead to a pronounced intensity drop at the number of He atoms that form this closed shell structure. Calculations by Coccia et al.[29,30] indicate that closed shell

dx.doi.org/10.1021/jp503179d | J. Phys. Chem. A 2014, 118, 6553−6559

anions such as OH^- and F^- are able to be solvated in ^4He droplets but interact too weakly with the He to lead to magic numbers in cluster size distributions. In contrast, H^- sits outside the droplets.[31] More recent calculations by Huber and Mauracher[32] suggest that the metastable anion He^{*-} strongly binds to He and prefers a position inside a ^4He droplet whereas the metastable dimer anion He_2^{*-} is heliophobic and weakly binds to the surface of a He droplet. However, the statistical uncertainty for the $He_m(CO_2)_nO^-$ anions does not allow the assignment of a shell closure at a certain number of He atoms, as reported recently for halogen anions.[28] Furthermore, the superposition of isobaric anions (both ^{12}C and ^{16}O are close in mass to a multiple of ^4He) as shown in the inset of Figure 1 provides another challenge to identify magic numbers in the anion series $He_m(CO_2)_nO^-$ ($n \geq 0$).

In the following we shall first consider electron attachment to CO_2@He in the electron energy range below 4 eV, observed on the non-decomposed tetramer ion $(CO_2)_4^-$ and recorded at high-electron-energy resolution of about ΔE = 0.1 eV (FWHM). Subsequently, we shall explore the entire energy range between threshold (near 0 eV) and 67 eV where the non-decomposed complexes $(CO_2)_n^-$ and the solvated ions $(CO_2)_nO^-$ are formed via a series of resonant processes.

Figure 2 presents a comparison of electron attachment to homogeneous CO_2 clusters (pristine CO_2, top) and electron attachment to CO_2@He (bottom panel), both observed on the tetramer ion $(CO_2)_4^-$. Apparently, the two clearly separated low-energy resonant features from pristine CO_2 do strongly overlap when going to CO_2@He. One has to keep in mind that the energy scale refers to the kinetic energy of the electrons in a vacuum. Entering the droplet substantially affects both the energy and nature of the excess electron. As discussed earlier in a study on electron capture by pure He droplets,[33] electron injection into the bottom of the conduction band in He requires an energy of 1.15 eV (V_0 = −1.15 eV) and subsequent formation of electron bubbles requires some additional activation energy. In light of that, one would expect a shift of about 1.6 eV to higher energies when going from pristine CO_2 to CO_2@He.

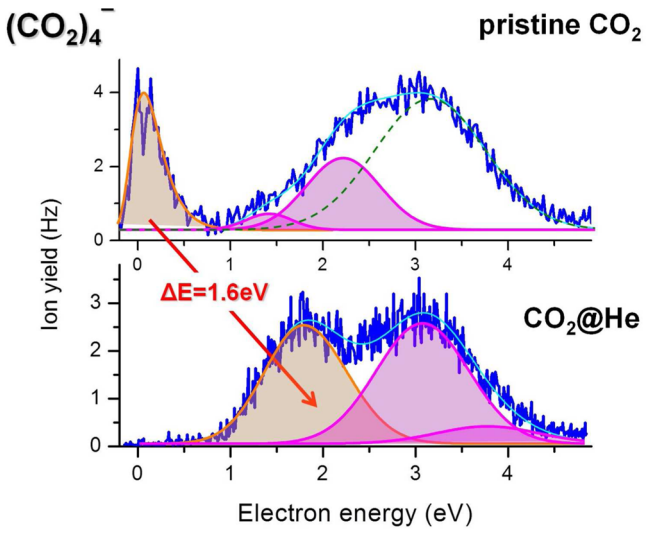

Figure 2. Comparison of electron attachment to homogeneous clusters of CO_2 (top) and CO_2@He (bottom) recorded at high-electron-energy resolution (ΔE = 0.1 eV, T_{He} = 10 K, p_{He} = 20 bar, I_{el} = 8 nA, p_{CO_2} = 6 mPa).

As discussed in detail in our recent study on electron attachment to CO_2 clusters,[26] the low-energy (<0.5 eV) ion signal is associated with a so-called *virtual* state near 0 eV[34,35] and the VFRs known from the ultrahigh-resolution experiments on electron attachment to CO_2 clusters.[24] This virtual state was introduced in the course of scattering experiments to describe excitation of the infrared inactive symmetric stretching mode in the threshold region. The feature between 1 and 4 eV consists of three overlapping resonances with maxima at 1.4, 2.2, and 3.1 eV. The resonance near 2.2 eV (not seen in electron attachment to single CO_2) can be assigned to a resonant scattering feature recently explored in electron scattering to single CO_2.[36] In CO_2, two quanta of the bending vibration (82.7 meV) are accidentally nearly degenerate with one quantum of the symmetric stretch vibration (165.8 meV). The coupling results in two vibrational states (a Fermi dyad) at 159 and 172 meV, each of them represents a mixing of bend vibration and symmetric stretch vibration. In the region between the virtual state and 2.5 eV (where no resonance mechanism was proposed so far) excitation of the higher member of the dyad exhibits a remarkable intensity with a broad resonant shape (indicative of a σ^* resonance[26]). Consequently, formation of the non-decomposed complexes in that energy region (Figure 2) was associated with this resonant scattering phenomenon.[36] The resonance feature with a maximum at 3.1 eV that was assigned to the $^2\Pi_u$ resonance, in the cluster environment shifted to lower energy by more than 1 eV.[26]

In general, formation of $(CO_2)_4^-$ from clusters at low energies (<5 eV) most likely proceeds via the reaction

$$e^- + (CO_2)_n \rightarrow (CO_2)_n^{-\#} \rightarrow (CO_2)_4^- + (n-4)CO_2 \quad (2)$$

with $(CO_2)_n^{-\#}$ the transient cluster anion formed upon electron attachment. The relaxation energy to form $(CO_2)_4^-$ can be used either to evaporate the target cluster (formation of $(n-4)$ neutral CO_2 molecules) or to split off the neutral complement of the target cluster ($(CO_2)_{n-4}$).

The fact that electron attachment to CO_2@He finally leads to $(CO_2)_n^-$ (with only small intensities of He containing ions), means that the droplet either undergoes complete evaporation in the course of the attachment process or splits off into a number of fragments, thereby releasing $(CO_2)_n^-$. To evaporate one He atom from the droplet, an energy of 0.6 meV is required, indicating that the complete evaporation of a target cluster (average size 10^5 He atoms) on average requires 60 eV, which in turn indicates that the target cluster does not completely evaporate. Open shell anions such as $(CO_2)_n^-$ may show a similar interaction with the superfluid He as a free electron, i.e., formation of a bubble and heliophobic character. Another possibility for large droplets is the high probability for two or more electrons entering the droplet and subsequent Coulomb repulsion between the dopant anion $(CO_2)_n^-$ and possible electron bubbles pushing all but one negatively charged species out of the droplet.

Figure 2 indicates that the low-energy contribution (<0.5 eV) and the higher energy feature (composed of contributions from the Fermi dyad) do overlap in CO_2@He having maxima at 1.8 and 3.1 eV. The first resonance shows the expected shift of about 1.6 eV and a substantial broadening, which prevents the observation of the doublet clearly seen from pristine CO_2

dx.doi.org/10.1021/jp503179d | J. Phys. Chem. A 2014, 118, 6553−6559

clusters. A two-Gaussian fit to the anion yield of the CO_2 tetramer anion from pristine CO_2 clusters as shown in ref 26 leads to peaks centered at 2.2 and 3.2 eV. However, these peaks do not lead to corresponding peaks in the CO_2@He case, shifted by 1.6 eV. The asymmetric peak shape suggests an additional contribution at the low-energy side, and by fitting the ion yield of the tetramer anion from pristine CO_2 clusters with three Gaussian peaks, we find for the CO_2@He corresponding peaks for the first two shifted by 1.6 eV. The width and the shifted position of the resonances agree very well for the two anion efficiency curves; however, the intensity of the resonances at higher electron energies are strongly suppressed for CO_2-doped He droplets. All resonances for dopant anions from doped He nanodroplets measured so far have shown a shift of about 1.6 eV, which supports the present approach to add an additional low-energy resonance. Measurements of anion efficiency curves from He nanodroplets doped with other species with high-electron-energy resolution are necessary to provide a clear answer for this unexpected behavior of the shift of the anion yield that is assigned to the Fermi dyad and the $^2\Pi_u$ resonance for $(CO_2)_n^-$ anions formed via electron attachment to pristine CO_2 clusters.

On the basis of the present material, one can tentatively interpret this rather unexpected result by supposing that in CO_2@He the contribution from the $^2\Pi_u$ resonance is strongly suppressed while the contribution from the Fermi dyad is mediated in CO_2@He, thereby extending to lower energies and finally resulting in a resonant feature peaking at 3.1 eV and a much weaker contribution at 3.8 eV. It should be noted that the scattering experiments on single CO_2 revealed effective excitation of the higher members of the Fermi dyad in the entire energy range between the virtual state and about 2.5 eV.

The relative intensities of the two contributions of the $(CO_2)_4^-$ anion efficiency curve are significantly affected when the nozzle temperature is changed between 10 and 11 K in the way that the ratio between the contributions at 1.8 eV to that at 3.1 eV (and 3.8 eV) is increased from 0.7 to 1.6. (Figure 3).

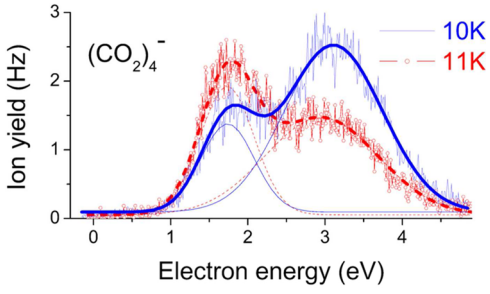

Figure 3. Electron attachment to CO_2@He leading to $(CO_2)_4^-$ at two nozzle temperatures (ΔE = 0.1 eV, p_{He}= 20 bar, I_{el} = 8 nA, p_{CO_2} = 6 mPa).

The increase of the nozzle temperature results in a decrease of the mean droplet size from about 1.4×10^5 to about 1.8×10^4 He atoms. This behavior may simply reflect the fact that the larger droplet provides better means to dissipate excess energy and hence the relative intensity of the higher energy resonance is increased with the size of the droplet.

The upper diagram of Figure 4 shows ion yield curves for the anion $(CO_2)_{10}^-$ (dashed line) and that of the complex $(CO_2)O^-$ (solid line) in an extended energy region up to 67 eV recorded with the low-electron-energy-resolution device.

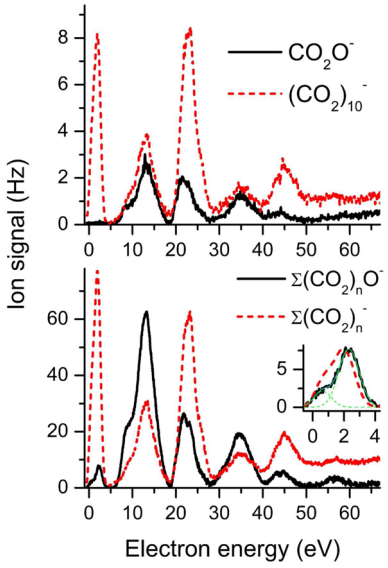

Figure 4. Ion yield of CO_2O^- (solid line) and the non-decomposed tetramer anion $(CO_2)_{10}^-$ (dashed line) in the extended electron energy range up to 67 eV recorded at low-electron-energy resolution (ΔE = 1 eV, T_{He} = 9.7 K, p_{He}= 23 bar, I_{el} = 45 μA, p_{CO_2} = 6 mPa). The lower diagram shows the sum of the anion yields of the series $(CO_2)_nO^-$ (solid line) and the series of the stoichiometric anion series $(CO_2)_n^-$ (dashed line). In the inset of the lower diagram the ion yield up to 4 eV for the two ion series is shown with the yield of the sum of the $(CO_2)_n^-$ anion series multiplied with 0.1 for a better comparison. Both curves can be reproduced by a two-Gaussian fit, as shown for the sum of the nonstoichiometric anion series (solid line).

The lower diagram shows the sum of the non-decomposed anions $(CO_2)_n^-$ (dashed line, n = 2−16) and the sum of the nonstoichiometric anions $(CO_2)_nO^-$ (solid line, n = 1−15). Resonant structures located near 2 eV (predominantly yielding the non-decomposed ions $(CO_2)_n^-$) as well as around 13, 22, 35, 44, and 57 eV are visible.

Negative ion formation within the first broad resonance can be associated with both low-energy features from Figure 2 (bottom), namely ion formation (a) via the virtual state and the vibrational Feshbach resonances and (b) via the Fermi dyad. Owing to the poor energy resolution, these two features are no longer separated. Whereas for CO_2O^- the 2 eV resonance is completely missing, fragment anions of larger clusters can be formed at this energy, although at much lower intensity than at higher electron energies. Furthermore, the 2 eV feature for both the stoichiometric and the nonstoichiometric CO_2 cluster anions exhibits two contributions at 0.6 and 2.3 eV with substantially higher intensity at the higher energy (see inset in the lower diagram of Figure 4). This suppression of the low-energy feature agrees very well with the temperature and pressure dependence reported for pristine $(CO_2)_4^-$ from pristine CO_2 clusters.[26] Taking into account space charging by the 45 μA electron beam, these two energies can be assigned to the resonances at 1.7 and 3.1 eV measured with high resolution (Figures 2 and 3). At these low energies the additional energy required to dissociate one CO_2 molecule is provided by the solvation of the anion in a large enough number of CO_2 molecules. In the present data we observe an increase of the red shift of the low-energy resonances with increasing cluster size and the feature seen at 0.6 eV in the inset of the lower panel of Figure 4 is only present for O^- that is solvated by more than five CO_2 molecules. Anion formation

dx.doi.org/10.1021/jp503179d | J. Phys. Chem. A 2014, 118, 6553−6559

within the second resonance feature peaking near 13 eV can be assigned to the electronically excited resonances known from single CO_2 (see relative cross section of O^- formation in ref 26) but also further electronically excited resonances that are known from condensed phase experiments. Electron stimulated desorption (ESD) of O^- from condensed phase CO_2 shows a series of strong resonances in the energy region above 10 eV.[37] One can assume that the surrounding He matrix substantially decreases the autodetachment of these excited resonances (not present in DEA to single molecules) to a degree that they become visible in the desorption of fragment anions.[38]

The third feature for negative ion formation around 22 eV roughly coincides with the energy range observed in the formation of negatively charged pure He droplets.[33] We accordingly propose that negative ion formation in that domain is mediated by electronic excitation of He, i.e., electronic excitation of He and attachment of the slowed down electron to CO_2. From the fact, however, that also DEA takes place (formation of $(CO_2)_nO^-$) we propose that in addition to capture of inelastically scattered low-energy electrons, two further mechanisms are operative, resulting in the formation of the solvated ion complexes, namely Penning ionization and DEA induced by coupling of CO_2 to *electron-exciton* complexes in He. Penning ionization of CO_2 via the He (1s2s) metastable states ^3S and ^1S creates electrons at energies in the range below 6 eV (depending on the amount of energy that remains in the CO_2 cluster) which can induce DEA in CO_2 molecules:[39,40]

$$e^-(22\ eV) + He \rightarrow He^* + e^-(2.2\ eV) \quad (3a)$$

$$He^* + (CO_2)_m \rightarrow He + (CO_2)_{m-i}^+ + (CO_2)_i + e^-(<6\ eV) \quad (3b)$$

$$(CO_2)_i + e^-(\sim 4\ eV) \rightarrow (CO_2)_nO^- + CO(CO_2)_{i-n-1} \quad (3c)$$

The second and probably dominant mechanism involves electron-exciton resonances, which are the condensed phase analogues to the well-known He^{*-} resonances with the lowest He^{*-} (1s2s2p) Feshbach resonance, located 0.5 eV below the lowest excited neutral, He(1s2s,^3S)

$$e^-(22\ eV) + He \rightarrow He^* + e^-(2.2\ eV) \rightarrow He^{*-} \quad (4a)$$

$$He^{*-} + (CO_2)_m \rightarrow He + (CO_2)_{m-n-1}CO^+ + (CO_2)_nO^- \quad (4b)$$

From electron stimulated desorption of molecules on rare gas films, these substrate mediated DEA processes can be observed as strong enhancements in the fragment ion desorption yield at the energy of the electron-exciton resonances.[41]

Anion formation within the feature around 35 eV can be considered in analogy to the processes discussed for the 13 eV resonance region, scaled to higher energy by the excitation energy of He. In other words, inelastic scattering from He leads to attachment of electrons in the energy range around 13 eV to CO_2 via electron excited resonances.

Figure 5 displays the intensity distributions of the series $(CO_2)_nO^-$ (open circles) recorded at 13 eV and that of $(CO_2)_n^-$ (solid squares) recorded at 2 eV electron energy. It should be noted that these spectra do not represent the raw data. All contributions from different isotopomers for a given anion were added up. In the anion spectrum obtained at 13 eV the peaks due to the stoichiometric anions and those due to products of the form $He_m(CO_2)_nO^-$ are suppressed. The inset

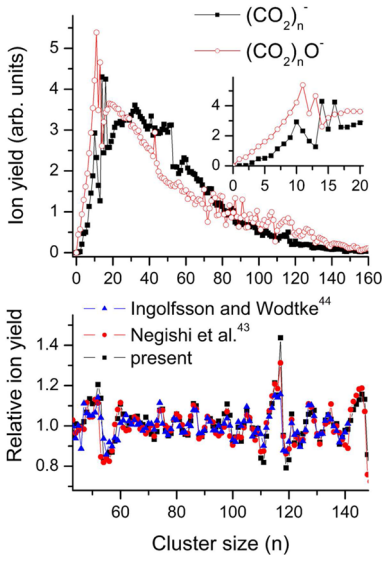

Figure 5. Intensity distribution of the non-decomposed complexes $(CO_2)_n^-$ recorded at 2 eV and that of the solvated ions $(CO_2)_nO^-$ recorded at 13 eV electron energy (T_{He} = 9.7 K, p_{He} = 23 bar, I_{el} = 45 μA, p_{CO_2} = 6 mPa). The distribution of the complexes $(CO_2)_n^-$ for $n <$ 4 essentially reflects their stability (see the text). Magic numbers in both anion series indicate unimolecular fragmentation after the ionization process, where weakly bound cluster anions are depleted relative to their neighboring cluster sizes. The lower diagram shows the relative ion intensities for $(CO_2)_n^-$, i.e., a difference of measured anion yields (upper panel) and a strongly smoothed fit to this curve in comparison to equally treated data published in the literature.[43,44]

in the upper panel of Figure 5 shows the ion yields for cluster sizes up to n = 20. Whereas the monomer anion CO_2^- cannot be found at all and the dimer $(CO_2)_2^-$ is only slightly larger than the noise, the trimer is clearly visible in the mass spectrum. High-level *ab initio* calculations predict that the tetramer is at the brink of stability.[42] We can therefore assume that the intensity distribution of $(CO_2)_n^-$ reflects the stability of these anions in the He droplet; i.e., the monomer and dimer may be metastable but the larger cluster anions do possess appreciable binding energies for the excess electron (positive electron affinities). Both cluster size distributions exhibit pronounced intensity anomalies (magic numbers) that are also known from cluster size distributions obtained via electron attachment to pristine CO_2 clusters.[43,44] To compare the present mass spectrum of the $(CO_2)_n^-$ anions with cluster size distributions published in the literature,[43,44] we plotted the difference of the measured anion yields and a strongly smoothed curve for the same data for all three series. Thereby intensity anomalies are more easily visible and can be compared for the three different experiments. All three data exhibit the same intensity anomalies in the cluster size range from n = 45 to 142 (where data from the two references have been published). It is interesting to note that Ingolfsson and Wodtke[44] assign the magic numbers to intensity anomalies of the neutral CO_2 clusters formed via supersonic expansion. They claim that 0 eV electron attachment does not heat up the clusters enough to lead to fragmentation, which is essential for the evolution of magic numbers. The present data, however, prove this explanation to be wrong as pickup of atoms and molecules into He droplets inevitably leads to a structureless neutral cluster size distributions as any excess energy by attaching an additional monomer will be carried away by the surrounding superfluid

dx.doi.org/10.1021/jp503179d | J. Phys. Chem. A 2014, 118, 6553−6559

He and boils off 1600 He atoms for each 1 eV of released energy. Thus, the magic numbers in the present experiment originate solely from the ionization process and it is interesting to note that even superfluid He is not able to carry away the excess energy that is released in the ionization event (even at the lowest electron energy of 2 eV).

In summary electron attachment to CO_2@He results in ionic complexes of the form $(CO_2)_n^-$ and $(CO_2)_nO^-$, similar to electron attachment to clusters of CO_2. The shape of the cross section for the formation of $(CO_2)_n^-$ indicates a substantial effect of the He environment indicating particular quenching and mediation process in CO_2@He, which have to be explored in more detail by additional studies at high-electron-energy resolution. The series of further resonances in the energy range up to 67 eV are due to (sequential) inelastic scattering of the electron from He and attachment of the slowed down electron leading to resonances 22 eV and multiples of 22 eV above the first resonance. The only exception is a strong resonance at 22 eV for the nonstoichiometric anions $(CO_2)_nO^-$, which does not have a counterpart at 2 eV at least for $n = 1$. Two processes where an intermediately formed He* leads to the non-stoichiometric anions $(CO_2)_nO^-$ at 22 eV are proposed as the inelastically scattered electron with its remaining kinetic energy of only 2 eV cannot lead to dissociative electron attachment to CO_2 clusters.

AUTHOR INFORMATION

Notes

The authors declare no competing financial interest.

ACKNOWLEDGMENTS

This work was supported by the Austrian Science Fund, Wien (FWF projects P23657, I978, P24443, P26635).

REFERENCES

(1) Zappa, F.; Denifl, S.; Mähr, I.; Bacher, A.; Echt, O.; Märk, T. D.; Scheier, P. Ultracold Water Cluster Anions. *J. Am. Chem. Soc.* **2008**, *130*, 5573−5578.

(2) Denifl, S.; Zappa, F.; Mähr, I.; Mauracher, A.; Probst, M.; Märk, T. D.; Scheier, P. Inelastic Electron Interaction with Chloroform Clusters embedded in Helium Droplets. *J. Am. Chem. Soc.* **2008**, *130*, 5065−5071.

(3) Mauracher, A.; Schöbel, H.; Ferreira da Silva, F.; Edtbauer, A.; Mitterdorfer, C.; Denifl, S.; Märk, T. D.; Illenberger, E.; Scheier, P. Electron attachment to trinitrotoluene (TNT) embedded in He droplets: complete freezing of dissociation intermediates in an extended range of electron energies. *Phys. Chem. Chem. Phys.* **2009**, *11*, 8240−8243.

(4) Denifl, S.; Zappa, F.; Mähr, I.; Lecointre, J.; Probst, M.; Märk, T. D.; Scheier, P. Mass Spectrometric Investigation of Anions Formed upon Free Electron Attachment to Nucleobase Molecules and Clusters Embedded in Superfluid Helium Droplets. *Phys. Rev. Lett.* **2006**, *97*, 043201.

(5) Ferreira da Silva, F.; Denifl, S.; Märk, T. D.; Ellis, A. M.; Scheier, P. Electron attachment to amino acid clusters in helium nanodroplets: Glycine, alanine, and serine. *J. Chem. Phys.* **2010**, *132*, 214306.

(6) Ferreira da Silva, F.; Bartl, P.; Denifl, S.; Märk, T. D.; Ellis, A. M.; Scheier, P. Formation of the 'magic' L-serine octamer in helium nanodroplets. *ChemPhysChem* **2010**, *11*, 90−92.

(7) Leidlmair, C.; Bartl, P.; Schöbel, H.; Denifl, S.; Probst, M.; Scheier, P.; Echt, O. On the possible presence of weakly bound fullerene−H_2 complexes in the interstellar medium. *Astrophys. J.* **2011**, *738*, L4.

(8) Denifl, S.; Zappa, F.; Mähr, I.; Ferreira da Silva, F.; Aleem, A.; Mauracher, A.; Probst, M.; Urban, J.; Mach, P.; Bacher, A.; Echt, O.; Märk, T. D.; Scheier, P. Ion−Molecule Reactions in Helium Nanodroplets Doped with C_{60} and Water Clusters. *Angew. Chem., Int. Ed.* **2009**, *48*, 8940−8943.

(9) Zöttl, S.; Kaiser, A.; Bartl, P.; Leidlmair, C.; Mauracher, A.; Probst, M.; Denifl, S.; Echt, O.; Scheier, P. Methane Adsorption on Graphitic Nanostructures: Every Molecule Counts. *J. Phys. Chem. Lett.* **2012**, *3*, 2598−2603.

(10) Zöttl, S.; Kaiser, A.; Daxner, M.; Goulart, M.; Mauracher, A.; Probst, M.; Hagelberg, F.; Denifl, S.; Scheier, P.; Echt, O. Ordered phases of ethylene adsorbed on charged fullerenes and their aggregates. *Carbon* **2014**, *69*, 206−220.

(11) Sulzer, P.; Rondino, F.; Ptasinska, S.; Illenberger, E.; Märk, T. D.; Scheier, P. Probing trinitrotoluene (TNT) by low-energy electrons. Strong fragmentation following attachment of electrons near 0 eV. *Int. J. Mass. Spectrom.* **2008**, *272*, 149−153.

(12) Bartl, P.; Tanzer, K.; Mitterdorfer, C.; Karolczak, S.; Illenberger, E.; Denifl, S.; Scheier, P. Electron ionization of different large perfluoroethers embedded in ultracold helium droplets: effective freezing of short-lived decomposition intermediates. *Rapid Commun. Mass Spectrom.* **2013**, *27*, 298−304.

(13) Sommerfeld, T.; Meyer, H.-D.; Cederbaum, L. S. Potential energy surface of the CO_2^- anion. *Phys. Chem. Chem. Phys.* **2004**, *6*, 42−45.

(14) Arnold, S. T.; et al. In *Photodetachment Spectroscopy of Negative Cluster Ions*; Scoles, G., Ed.; North Holland: Amsterdam, 1989.

(15) Burrow, P. D.; Sanche, L. Elastic Scattering of Low-Energy Electrons at 180° in CO_2. *Phys. Rev. Lett.* **1972**, *28*, 333−336.

(16) Boness, M. J. W.; Schulz, G. J. Vibrational excitation in CO_2 via the 3.8-eV resonance. *Phys. Rev. A* **1974**, *9*, 1969−1979.

(17) Christophorou, L. G.; McCorkle, D. L.; Christodoulides, A. A. Electron Attachment Processes. In *Electron-Molecule Interactions and Their Applications*; Christophorou, L. G., Ed.; Academic Press: Orlando, 1984.

(18) Dressler, R.; Allan, M. Energy partitioning in the O^-/CO_2 dissociative attachment. *Chem. Phys.* **1985**, *92*, 449−455.

(19) NIST Chemistry WebBook, http://webbook.nist.gov/.

(20) Klots, C. E.; Compton, R. N. Electron attachment to carbon dioxide clusters in a supersonic beam. *J. Chem. Phys.* **1977**, *67*, 1779−1780.

(21) Klots, C. E.; Compton, R. N. Electron-attachment to van der Waals polymers of carbon dioxide and nitrous oxide. *J. Chem. Phys.* **1978**, *69*, 1636−1643.

(22) Stamatovic, A.; Leiter, K.; Ritter, W.; Stephan, K.; Märk, T. D. Electron attachment to carbon dioxide clusters at very low electron energies. *J. Chem. Phys.* **1985**, *83*, 2942−2946.

(23) Knapp, M.; Echt, O.; Kreisle, D.; Märk, T. D.; Recknagel, E. Formation of long-lived CO_2^-, N_2O^-, and their dimer anions, by electron attachment to van der Waals clusters. *Chem. Phys. Lett.* **1986**, *126*, 225−231.

(24) Leber, E.; Barsotti, S.; Fabrikant, I. I.; Weber, J. M.; Ruf, M.-W.; Hotop, H. Vibrational Feshbach resonances in electron attachment to carbon dioxide clusters. *Eur. Phys. J. D* **2000**, *12*, 125−131.

(25) Fabrikant, I. I.; Hotop, H. Theory of Electron Attachment to CO_2 Clusters. *Phys. Rev. Lett.* **2005**, *94*, 063201.

(26) Denifl, S.; Vizcaino, V.; Märk, T. D.; Illenberger, E.; Scheier, P. High resolution electron attachment to CO_2 clusters. *Phys. Chem. Chem. Phys.* **2010**, *12*, 5219−5224.

(27) Muigg, D.; Denifl, G.; Stamatovic, A.; Echt, O.; Märk, T. D. High-resolution electron ionization study of CO, $(CO)_2$ and $(CO)_3$: appearance energies and bond dissociation energies. *Chem. Phys.* **1998**, *239*, 409−416.

(28) Ferreira da Silva, F.; Waldburger, P.; Jaksch, S.; Mauracher, A.; Denifl, S.; Echt, O.; Märk, T. D.; Scheier, P. On the size of ions solvated in helium clusters. *Chem.—Eur. J.* **2009**, *15*, 7101−7108.

(29) Coccia, E.; Marinetti, F.; Bodo, E.; Gianturco, F. A. Anionic microsolvation in helium droplets: OH^-He_n structures from classical and quantum calculations. *J. Chem. Phys.* **2008**, *128*, 134511.

(30) Coccia, E.; Marinetti, F.; Bodo, E.; Gianturco, F. A. Chemical solutions in a quantum solvent: Anionic electrolytes in ^{4}He nanodroplets. *ChemPhysChem* **2008**, *9*, 1323−1330.
(31) Sebastianelli, F.; Di Paola, C.; Baccarelli, I.; Gianturco, F. A. Quantum and classical structures for ^{4}He clusters with the H^- impurity. *J. Chem. Phys.* **2003**, *119*, 8276−8288.
(32) Huber, S. E.; Mauracher, A. On the formation of (anionic) excited helium dimers in helium droplets. *Mol. Phys.* **2013**, *112*, 794−804.
(33) Henne, U.; Toennies, J. Electron capture by large helium droplets. *J. Chem. Phys.* **1998**, *108*, 9327−9338.
(34) Kochem, K. H.; Sohn, W.; Hebel, N.; Jung, K.; Erhardt, H. Elastic electron scattering and vibrational excitation of CO_2 in the threshold energy region. *J. Phys. B: At. Mol. Phys.* **1985**, *18*, 4455−4467.
(35) Morgan, L. A. Virtual states and resonances in electron scattering by CO_2. *Phys. Rev. Lett.* **1998**, *80*, 1873−1875.
(36) Allan, M. Selectivity in the Excitation of Fermi-Coupled Vibrations in CO_2 by Impact of Slow Electrons. *Phys. Rev. Lett.* **2001**, *87*, 033201.
(37) Rowntree, P.; Sambe, H.; Parenteau, L.; Sanche, L. Formation of anionic excitations in the rare gas solids and their coupling to dissociative states of adsorbed molecules. *Phys. Rev. B* **1993**, *47*, 4537−4554.
(38) Illenberger, E. Formation and evolution of negative ion resonances at surfaces. *Surf. Sci.* **2003**, *528*, 67−77.
(39) Hotop, H.; Kolb, E.; Lorenzen, J. The temperature dependence of penning ionization electron energy spectra: He(2^3S) − Ar, N_2, NO, O_2, N_2O, CO_2. *J. Electron Spectrosc. Relat. Phenom.* **1979**, *16*, 213−243.
(40) Maruyama, R.; Tanaka, H.; Yamakita, Y.; Misaizu, F.; Ohno, K. Penning ionization electron spectroscopy of CO_2 clusters in collision with metastable rare gas atoms. *Chem. Phys. Lett.* **2000**, *327*, 104−110.
(41) Weik, F.; Illenberger, E. Dissociative electron attachment and charging of SF_6 adsorbed on rare gas films. *J. Chem. Phys.* **1998**, *109*, 6079−6085.
(42) Tsukada, M.; Shima, N.; Tsuneyuki, S.; Kageshima, H.; Kondow, T. Mechanism of electron attachment to van der Waals clusters: Application to carbon dioxide clusters. *J. Chem. Phys.* **1987**, *87*, 3927−3933.
(43) Negishi, Y.; Nagata, T.; Tsukuda, T. Structural evolution in $(CO_2)_n$ clusters ($n < 10^3$) as studied by mass spectrometry. *Chem. Phys. Lett.* **2002**, *364*, 127−132.
(44) Ingolfsson, O.; Wodtke, A. M. Electron attachment time-of-flight mass spectrometry reveals geometrical shell closings in van der Waals aggregates. *J. Chem. Phys.* **2002**, *117*, 3721−3732.